Electrochemical determination of ferrocene diffusion coefficient in liquid media under high CO_2 pressure: Application to DMF–CO_2 mixtures

S. Chanfreau, P. Cognet *, S. Camy, J.-S. Condoret

Laboratoire de Génie Chimique, Site Basso-Cambo, 5 rue Paulin Talabot, BP 130, 31106 Toulouse cedex 1, France

Abstract

Electrochemical method can be useful for the determination of diffusion coefficients in various media. For low polarity media, ultramicroelectrodes are preferably used. In this work, the electro-oxidation of ferrocene has been studied in dimethylformamide (DMF)–CO_2 mixtures under various CO_2 pressures, using a 100 μm diameter Pt microelectrode. Tetrabutylammonium perchlorate (TBAP) was chosen as the supporting electrolyte. Cyclic voltammetry was used in order to obtain values of diffusion coefficient of ferrocene, which were determined by using the Randles–Sevcik relation. This method proved to be convenient in such low polarity solvent. In addition, fluid phase equilibria of CO_2–DMF mixtures were calculated and pressure–composition phases diagrams were established for the concerned binary mixtures, thanks to commercial Prophy Plus™ software (Prosim S.A., France). So, both liquid phase expansion, due to swelling by high-pressure CO_2 and effective bulk concentration of ferrocene were estimated. Nevertheless, electrochemical measurements were problematic when high-pressure single phase conditions of CO_2–DMF mixtures were reached.

Keywords: CO_2–DMF mixtures; Pressure–composition phase equilibrium; Ferrocene; Randles–Sevcik relation; Microelectrode; Diffusion coefficients; Tetrabutylammonium perchlorate

1. Introduction

Liquid or supercritical CO_2 is nowadays considered as a promising alternative to the use of toxic organic solvents. As high-pressure technology is mastered, the use of rich CO_2 media is of great interest for designing green processes. Then, the estimation of mass transfer properties in these new media becomes crucial for process design. Unfortunately, very few data have been reported concerning the measurement of diffusion coefficients in these media. Electrochemical methods are widely used for the determination of diffusion coefficients of electroactive species in polar media but this technique is more difficult to apply to low polarity media. Carbon dioxide has a very low dielectric constant ($\varepsilon(scCO_2) = 1.6$, [1]). So, using liquid or supercritical CO_2 as a reaction or extraction medium often requires the addition of a polar co-solvent to enhance solubility of electrolytic species. In these media, various CO_2 concentrations can be obtained by applying different CO_2 pressures up to supercritical conditions. Diffusion coefficients were rarely determined by an electrochemical way when media are subjected to high pressures because conventional electrochemical techniques, such as polarography or rotating disc electrode, are uneasy to operate in a high-pressure apparatus. Nevertheless, voltammograms of several metallic ions were obtained with a mercury electrode under high-pressure and high temperature conditions [2]. On the other hand, ultramicroelectrodes have gained in interest due to their multiple applications. Contrary to conventional electrodes, mass transfer at an ultramicroelectrode achieves a hemispherical concentration profile, corresponding to

* Corresponding author. Tel.: +33 (0) 5 34 61 52 60; fax: +33 (0) 5 34 61 52 53.
E-mail address: Patrick.Cognet@ensiacet.fr (P. Cognet).

radial diffusion [3]. The use of microelectrodes allows the measurement of low faradaic currents, even in solutions of low ionic strength because the ohmic drop remains very low [4].

In this work, we propose to perform electrochemical measurements in a CO_2–dimethylformamide (DMF) mixture, using ferrocene as the electroactive species. Furthermore, DMF is a good example of a polar aprotic solvent. Indeed, such solvents are required to minimize protonation reactions during organic syntheses [5]. The ferrocence/ferricinium couple is often chosen because it exhibits high electron transfer rate. Tetrabutylammonium perchlorate was used as supporting electrolyte. Electrocarboxylation using CO_2 under atmospheric pressure has been widely studied in such a solvent ([6–9]). It was also recently studied in liquid pressurised CO_2–DMF mixture [10].

2. Determination of diffusion coefficients by electrochemical methods in high-pressure CO_2–DMF mixtures

2.1. Transient conditions and steady-state conditions

In experiments with time scales on the order of 1 V s^{-1}, voltammograms obtained with ultramicroelectrodes differ from those obtained using electrodes of conventional size, because differences in mass transfer within the diffusion layer. At large electrodes, mass transfer occurs mostly perpendicularly to the surface (planar diffusion), leading to a typical peak-shaped voltammogram [11]. For a reversible redox process, the peak current obeys the Randles–Sevcik relationship (1).

$$I_p = 0.4463(F^3(RT)^{-1})^{1/2} n^{3/2} A D^{1/2} c v^{1/2} \quad (1)$$

where I_P is peak current (A), F is Faraday's constant (C), T is the temperature (K), R is the gas constant (J mol^{-1} K^{-1}), n is the number of exchanged electrons, A is the electrode area (cm^2), v is the potentiostat scan rate (V s^{-1}), D the diffusion coefficient (cm^2 s^{-1}) and c the bulk concentration (mol cm^{-3}) of the electroactive species [12]. This relation can only be applied with reversible systems and with no adsorption phenomenon at the electrode. It is widely used for the determination of diffusion coefficients.

Conversely, mass transport at ultramicroelectrodes induces a hemispherical concentration profile (radial diffusion), leading to a steady-state sigmoidal voltammogram [4]. A microelectrode is defined as any electrode having at least one dimension with a size of less than 25 μm [13]. When the size of the electrode is reduced, the most characteristic feature is the effect of non planar diffusion towards the electrode surface. Unlike conventional electrodes, currents generated at ultramicroelectrodes do depend on their geometry according to Eq. (2), only valid in steady state conditions:

$$I_L = anFDcr \quad (2)$$

in which $a = 4\pi$ for a sphere, 2π for a hemisphere and 4 for a disc. I_L is the limiting current (A) and r is the microelectrode radius (cm). The diffusion coefficients for electroactive species in a reversible system are obtained by exploiting sigmoid-shaped voltammograms, providing that no adsorption phenomenon occurs at the working electrode [14].

As a consequence, the diffusion mode depends on the size of the working electrode. So, the Randles–Sevcik relationship can be applied when planar diffusion occurs for a reversible redox process. However, it may be possible that planar diffusion is not the only mass transfer mode. So, transient conditions can be observed when intermediate size electrodes are used.

2.2. Intermediate size electrodes

Low duration and therefore frequent replacement of ultramicroelectrodes are reported due to their brittleness. To alleviate this drawback, larger microelectrodes can be used. So, planar and non planar diffusion modes occur simultaneously and a spherical correction may be added, depending on the size of the electrode. As a consequence, the complete peak current relationship is written as follows (3) [12]:

$$I_P = \underbrace{0.4463(F^3(RT)^{-1})^{1/2} n^{3/2} A D^{1/2} c v^{1/2}}_{\text{I(plane)}} + \underbrace{0.7516\, nFADcr^{-1}}_{\text{I(spherical correction)}} \quad (3)$$

in which r is the disc-shaped microelectrode radius. Meanings of other symbols have already been given.

As it is revealed in the relationship (3), spherical correction current depends on the electroactive species bulk concentration and mostly on microelectrode dimension at any scan rate. It is also indirectly influenced by temperature effect through the diffusion coefficient. Like already quoted relation, it can only be applied to reversible systems, with no adsorption phenomenon at the electrode.

On a first approximation, the shapes of experimental voltammograms can be useful to identify the main diffusion mode. But it is also validated by the criterion θ ($\theta = D\,t\,r^{-2}$), where t is electrolyse time). Thus, radial diffusion is occurred when θ is much smaller than 1.

In addition, usual electrochemical parameters can be calculated in order to classify electron process at the electrode. So, the $E_{1/2}$ half-reaction potential ($E_{1/2} = (E_{forward} + E_{backward})/2$), the RI_P peak current ratio ($RI_P = -I_{Pbackward}/I_{Pforward}$), the ($E_P - E_{P/2}$) separation potential difference ($E_P - E_{P/2} = E_{Pforward} - E_{Pforward/2}$) or the ΔE_P potential difference ($\Delta E_P = E_{forward} - E_{backward}$) was obtained from the cyclic voltammograms.

2.3. Simulation of liquid phase expansion

For the calculation of the diffusion coefficient of ferrocene in high-pressure CO_2–DMF mixtures, ferrocene concentration was assumed to be negligible in the light (vapour) phase. Nevertheless, it was necessary to estimate the effective bulk concentration of ferrocene in the liquid

phase, and, therefore, to evaluate liquid phase expansion due to swelling by high-pressure CO_2. Thus, phase diagrams have been established for the binary mixture CO_2–DMF, thanks to commercial Prophy Plus^{TM} software (Prosim S.A., France).

In these calculations, neither ferrocene nor TBAP were taken into account. Fluid phase equilibria for the CO_2–DMF mixture have been computed by using the Soave–Redlich–Kwong (SRK) [15] state equation, and, in order to account for interactions taking place between components into the mixture, we used the mixing rules developed by Huron and Vidal and Huron [16] and modified by Michelsen [17] (MHV2 mixing rules). The UNIQUAC [18] activity coefficients model has been chosen to determine the value of the free excess Gibbs energy needed in the calculation of the mixture parameters. In this case, it is necessary to know the value of binary interaction parameters A_{ij} and A_{ji} for the CO_2–DMF mixture. These parameters have been obtained by fitting experimental results of the literature [19] thanks to the commercial software Pro-Reg^{TM} (Prosim S.A., France). $A_{CO_2\text{–DMF}}$ and $A_{DMF\text{–}CO_2}$ were estimated at -330.605 cal mol^{-1} and 719.474 cal mol^{-1}, respectively. A comparison of experimental and calculated vapour–liquid equilibria is presented in Fig. 1. As it can be seen from this figure, experimental points are quite well described by the model. Theses curves show mono and two phase domains.

Indeed, according to the initial amount of DMF and the applied pressure, a CO_2–DMF mixture can be either a single or a two phase system. In the latter case, the theoretical composition of each phase, as well as the volume of each phase inside the high-pressure cell can be reasonably estimated using the SRK-MHV2-UNIQUAC model described above.

For example, as it can be seen on Fig. 1, at 78 bar and 313.05 K, CO_2 is the major component in both phases:

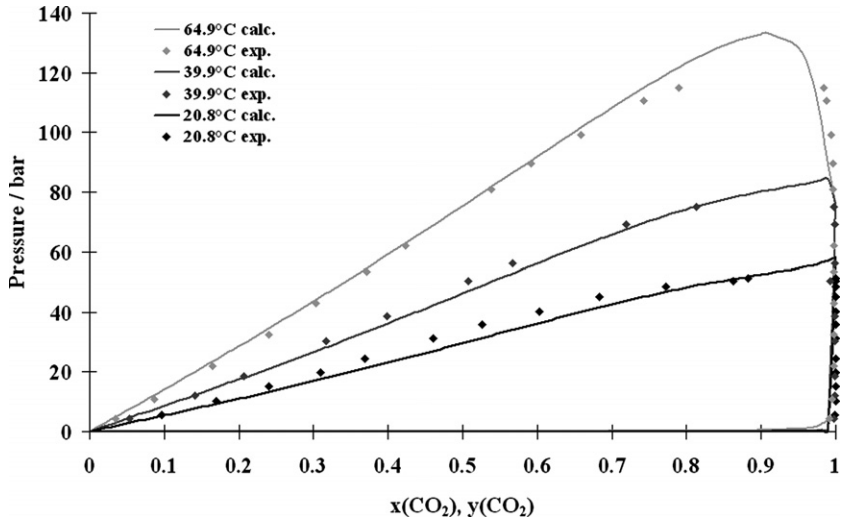

Fig. 1. Comparison of experimental [19] and calculated *P-x,y* phase equilibrium CO_2–DMF mixtures at different temperatures.

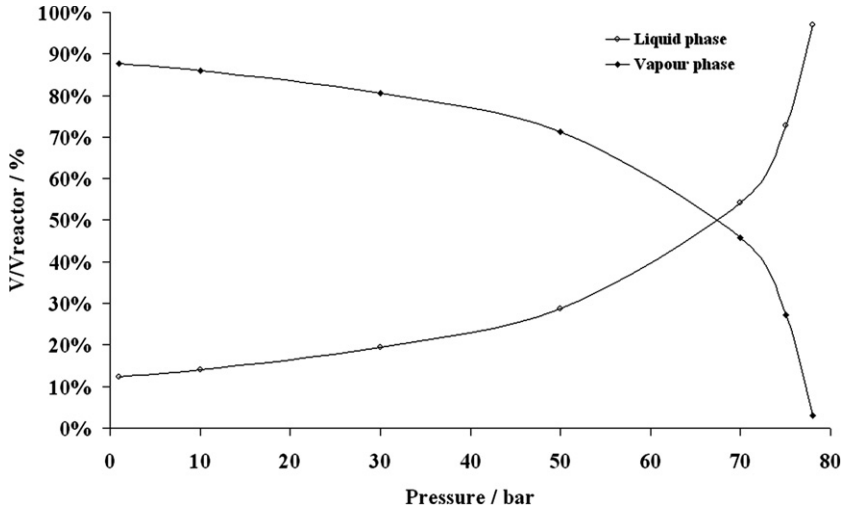

Fig. 2. Volume of phases evolution inside the reactor according to the applied pressure. $T = 39.9$ °C, $m_{DMF} = 24$ g.

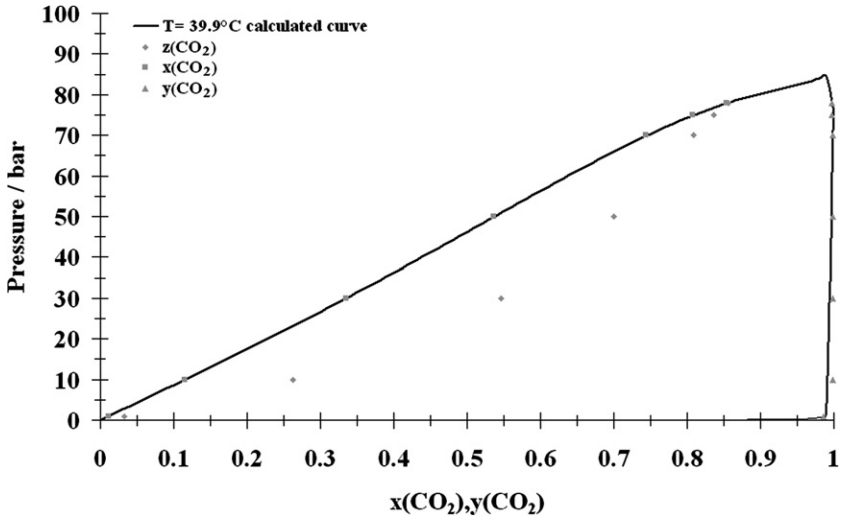

Fig. 3. CO_2–DMF *P-x,y* phase equilibrium at 39.9 °C. Calculated initial mixing points ($z(CO_2)$) and compositions of liquid and vapour phases at equilibrium ($x(CO_2)$; $y(CO_2)$) inside the reactor ($m_{DMF} = 24$ g).

85.38% in the liquid phase and 99.77% in the vapour phase. DMF concentration is higher in the liquid phase but it is highly diluted whatever the phase.

In the two phase operation zone, actual electroactive species concentration in the liquid phase must be recalculated, taking into account the liquid phase expansion (Fig. 2). Volume of the heavy phase (DMF rich phase) can be estimated thanks to PROPHY Plus™ software from calculation of the vaporization ratio, corresponding to initial amounts of DMF and CO_2 introduced in the reactor of known total volume and the temperature. For example, as we can see on Figs. 2 and 3, vapour phase volume can be neglected for the CO_2–DMF mixture used at 78 bar.

So, the Randles–Sevcik relation was applied. As an assumption, Ferrocene concentration calculations were run assuming that no ferrocene was present in the CO_2 rich light phase, whatever the applied pressure.

3. Experimental

3.1. Reagents

Ferrocene (Fluka, 98% purity) and TBAP (Fluka, electrochemical grade 99% purity) were used as received. DMF (Sigma–Aldrich, 99.9% purity) was dried over molecular sieves before use. CO_2 plunging tube bottle was provided by Air Liquide. All the freshly prepared solutions were degassed under CO_2 gas flow before experiments.

3.2. High-pressure electrochemical cell

A 250 mL thermostated jacketed vessel made of stainless steel was used (Parr Instrument Company, USA). Removable glass liner could be used in order to isolate the reaction medium from the metallic parts. As a consequence, volume was reduced to 150 mL. Moreover, two sapphire portholes, facing each other, allowed observation inside the reactor. CO_2 was supplied by a pneumatic pump (Top industrie, France) equipped with a pressure regulation. Temperature was measured with a thermometer probe (temperature scale: $-10 + 70$ °C $\pm$ 1 °C) and pressure was measured thanks to a Bourdon tube type manometer (pressure scale: 0–350 $\pm$ 5 bar).

3.3. Electrodes-electrochemical apparatus

A three electrode system was chosen to carry out experiments in a single cell reactor. A 100 μm diameter platinum wire (Goodfellow) sealed in a 3 mm diameter glass tube was used as the working electrode. It was polished with 0.3 μm roughness abrasive band before each experiment. The counter-electrode was a platinized titanium grid (2×2 cm approx.). A silver wire pseudo-reference electrode (Goodfellow, 99.99% purity 1 mm diameter) was fixed near the working electrode glass. PTFE electric crossing device made it possible to ensure the sealing of the reactor.

Voltamperometric measurements were run on a Voltalab 32 potentiostat (Radiometer, France).

3.4. Procedure

Solutions of TBAP (25 mL) and ferrocene in DMF at 0.1 M and 10^{-3} M concentrations respectively were first prepared before each experiment. Then, at atmospheric pressure, the glass liner was filled with the solution and set inside the stainless steel vessel. Otherwise, under high-pressure conditions, only the stainless steel vessel was filled with the solution.

The reactor was then closed and the solution was degassed by bubbling CO_2 until a 5 bar inside pressure is attained. Then, the vessel was slowly depressurised to atmospheric pressure. Finally, pressure was increased to the

desire value. This should be gradual from 5 to 5 bar when a high-pressure was aimed.

4. Results and discussion

4.1. Preliminary studies at atmospheric pressure

Experiments were first run under atmospheric conditions to test the applicability of the Randles–Sevcik relation with our experimental setup. Ferrocene diffusion coefficients were determined at $T = 26$ °C. Peak intensities were obtained at several potential scan rates. Fig. 4 shows peak intensities represented as a function of the square root of the scan rate. A straight line is obtained, showing that the electrochemical process is diffusion controlled. Diffusion coefficient was first calculated from the slope of the straight line, according to Eq. (1). Reproducibility was verified by several measurement runs. Diffusion coefficient of ferrocene was determined from minimization of differences between experimental and modelling peak intensities values (Fig. 4). Reduced species diffusion coefficient was found to be close to literature values [20,21] ($D = 10^{-5}$ cm^2 s^{-1}). Thus the order of magnitude is in good agreement and the several experimental data are close for a $\pm 10^{-6}$ cm^2 s^{-1} uncertainty.

So, planar diffusion is not the only involved mass transport mode and the residual intensity observed is explained both by spherical diffusion contribution and by taking into account a charging current (I_c) which varies with v [12,22]. The spherical contribution current was estimated at 1.16×10^{-8} A cm^{-2}.

Thus, spherical corrections and capacitive currents must be considered when studies are run under high scan rates in non conventional media. In particular it must be considered in CO_2 high-pressure solutions for diffusion coefficients determination. The whole experimental device was proved to be suitable for such studies.

4.2. Determination of diffusion coefficients under CO_2 high pressure

To apply relation (3), accurate bulk concentration knowledge is needed. Thus, the liquid phase volume expansion was evaluated according to the applied pressure as described in Section 2.3.

Peak-shaped voltammograms were obtained at moderated scan rates, indicating planar diffusion mode. Cyclic voltammetries were run under several CO_2 applied pressure. Peak intensity resolutions were satisfying but reduction peak heights were found difficult to be estimated (Fig. 5).

At high scan rates, it can be observed that measurement noise appears. Oxidation peak potential remains almost constant as potential scan rate is increased, as expected for a non limiting electron transfer.

The ($E_P - E_{P/2}$) separation values are higher than predicted by theory ($E_P - E_{P/2}$ *ca.* 59.4 mV at 40 °C). This potential difference increases with pressure until 60 bar (Table 1). This can be linked to the ohmic drop. Then, the ($E_P - E_{P/2}$) potential difference is slow down at a 70 bar pressure, resulting from the high CO_2 enrichment of the solution. $E_{1/2}$ half-reaction potential values vary in the same way. On the other hand, ΔE_P continuously increases with pressure. As CO_2 pressure increases, the volume of solution also increases. Then, TBAP concentration decreases and the ohmic drop increases. This could explain the variation of peak separation. Finally, the system seems to be reversible at lower pressure (RI_P *ca.* 1) and it appears as quasi-reversible when higher pressures are applied (RI_P *ca.* 0.90).

Diffusion coefficients were calculated for each pressure value. Fig. 6 shows the evolution of the diffusion coefficient with pressure. It can be observed that its estimated value increases with pressure until 60 bar. Indeed, viscosity of

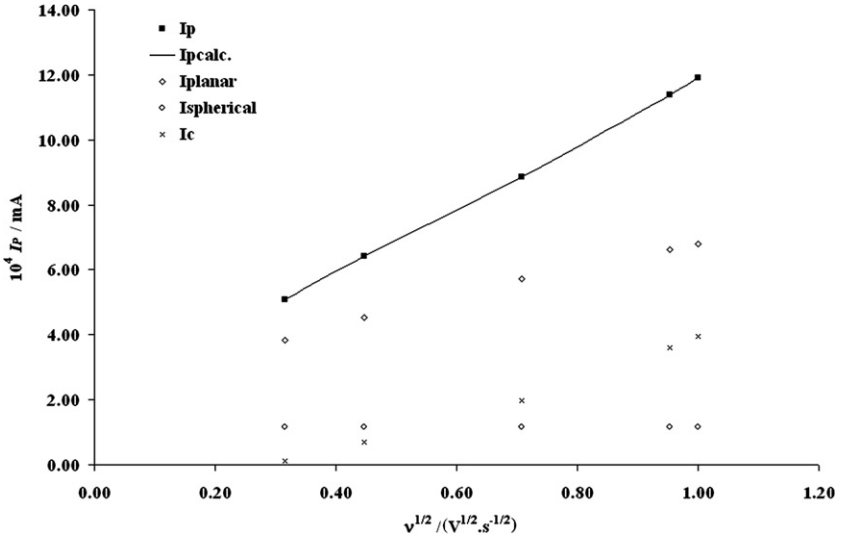

Fig. 4. Ferrocene coefficient diffusion determination using Randles–Sevcik modified relationship in DMF–TBAP solution with a Pt microelectrode ($r = 50$ μm) by cyclic voltammetry under atmospheric pressure. [TBAP] = 0.1 M, [Fc] = 10^{-3} M, $T = 26$ °C.

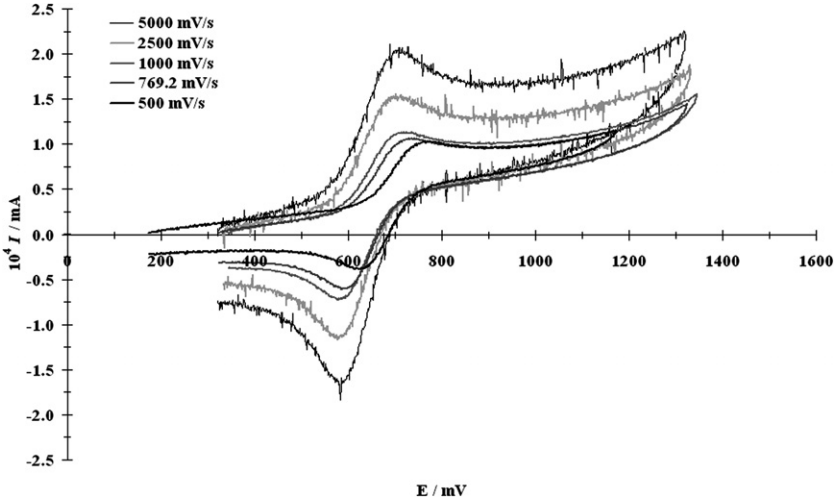

Fig. 5. Cyclic voltammetry of ferrocene at several scan rates. $n_{Fc} = 2.6 \times 10^{-2}$ mmol, $n_{TBAP} = 2.5$ mmol. $T = 40$ °C, $P = 70$ bar.

Table 1
Cyclic voltammetry data of ferrocene (Fc) in TBAP/DMF media according to the CO_2 applied pressure

Pressure (bar)	Forward scan				Backward scan		RI_p	$E_{1/2}$ (mV)	$(E_p - E_{p/2})$ (mV)	$(E_p - E_{p/2})$ (theor) (mV)	ΔE_p (mV)	ΔE_p (theor) (mV)
	$10^{-4} I_p$ (mA)	E_p (mV)	$10^4 I_{p/2}$ (mA)	$E_{p/2}$ (mV)	E_p (mV)	$10^{-4} I_p$ (mA)						
10	1.32	686	0.71	619	604	−1.27	0.96	645	67	58.8	82	61.5
20	1.43	729	1.34	654	634	−1.28	0.89	682	75	59.0	95	61.7
50	2.65	742	1.66	662	634	−2.28	0.86	688	98	59.2	108	61.9
60	3.43	725	2.32	647	614	−2.76	0.80	670	104	59.4	111	62.1
70	1.13	718	0.61	633	579	−1.04	0.92	649	85	59.4	139	62.1

$v = 1000$ mV s^{-1}. Initial liquid phase parameter: $V = 25$ mL, [TBAP] = 0.1 M and [Fc] = 10^{-3} M.

the liquid phase decreases because of CO_2 enrichment, favouring ferrocene diffusion in the medium.

At a 70 bar pressure, CO_2–DMF mass ratio is close to 1.75. At this point, lower ferrocene concentrations are then involved and measurement noise increases, leading to a bad accuracy in the determination of the peak intensity. In addition, a decrease of the measured intensity values was observed. Indeed, ferrocene was found to be soluble in supercritical CO_2 (2.07×10^{-3} g mL^{-1}, $P = 97.5$ bar, $T = 40$ °C) [22]. So, the ferrocene concentration in the

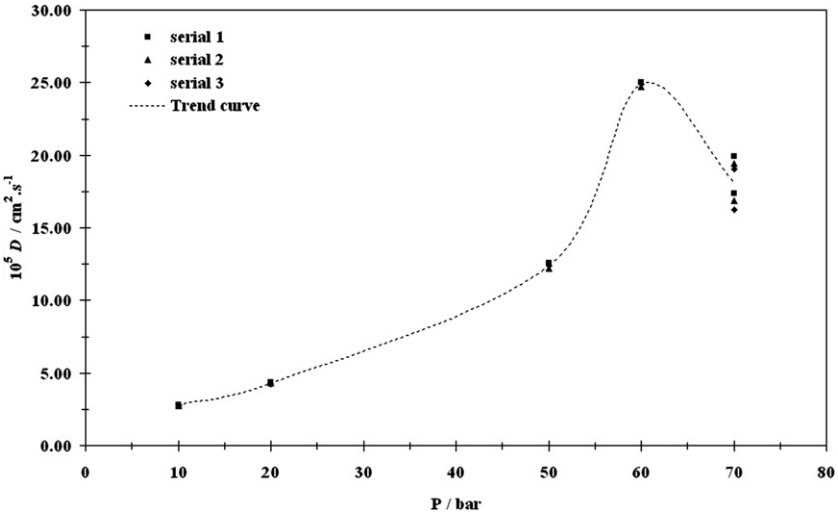

Fig. 6. Ferrocene diffusion coefficients in CO_2–DMF media according to applied pressure for two groups of three measurement series. Initial liquid phase parameter: $V = 25$ mL, [TBAP] = 0.1 M and [Fc] = 10^{-3} M, $T = 40$ °C.

Table 2
Diffusion coefficients of ferrocene under supercritical conditions in several media

T (°C)	P (bar)	Electrolytical media	D ($cm^2\ s^1$)	Ref.
38	121.6	Water in CO_2 emulsion	2.50×10^{-7}	[26]
80	89.6	CO_2 with added $[H_2O] = 55$ mM	2.90×10^{-4}	[5]
80	89.6	CO_2 with $[THAPF_6]$[a] $= 0.05$ M and $[H_2O] = 0.13$ M	1.00×10^{-4}	[27]
80	90.2	CO_2 with $[THAPF_6]$[a] $= 0.01$ M and $[H_2O] = 0.13$ M	2.75×10^{-4}	[27]
25	52	CDFM[b] with [TBATFB][c] $= 8$ mM	2.36×10^{-5}	[28]
115	90	CDFM[b] with [TBATFB][c] $= 8$ mM	1.30×10^{-4}	[28]
275	125	Acetomtrile with $[CF_3SO_3Na]$[d] $= 0.11$ M	2.40×10^{-4}	[21]

[a] $THAPF_6$: tetrahexylammmonium hexafluorophosphate.
[b] CDFM: chlorodifluoromethane.
[c] TBATFB: tetra-*n*-butylammonium tetrafluoroborate.
[d] CF_3SO_3Na: sodium tiifluoromethanesulfonate.

heavy phase was maybe overestimated and its solubility in the light phase should have been taking into account as the pressure was raised. Nevertheless, the ferrocene partition coefficient was hard to obtain under these extreme experimental conditions. Near the single phase point, the chosen electrochemical method appears unsuitable for the determination of the ferrocene diffusion coefficient. This was already observed in acetonitrile [23], where decreasing intensity values were attributed to the solvent properties of near-critical and supercritical fluids.

No experiment could be carried out at the single phase point. No signal was recorded because TBAP is only slightly soluble in the CO_2 rich solution and precipitation was observed. Difficulty in measuring of diffusion coefficients in such medium is confirmed in literature since very few diffusion coefficients obtained in similar media are tabulated. More polar solvents are rather used for ferrocene diffusion study (Table 2) and medium conductivity is often improved by adding water at high temperature.

5. Conclusions

Estimation of diffusion coefficient of a Nernstian reversible system was carried out in a non conventional medium such as CO_2–DMF mixture, for different CO_2 pressures. Planar diffusion mode was established for operating conditions close to CO_2–DMF mixture subcritical conditions. The most important result seems to be the increase of the diffusion coefficient value as CO_2 pressure increases. For example, we observed a five-fold increase at 60 bar, compared to 10 bar. The lack of results at the one phase point might be resolved by the use of a new support electrolyte. Two kinds of compounds could be tested. First, very hydrophobic salts were studied to ensure electrical conductivity in non-polar media [24]. Secondly, some ionic liquids are known to be able to solubilize large amounts of CO_2 [25]. Water-in-supercritical CO_2 microemulsions have also been used [26,5,27].

This preliminary study, carried out using an aprotic polar solvent, aimed at evaluating the ability to carry out aromatic halide electrocarboxylation under supercritical CO_2 conditions [29]. The very low dielectric constant of CO_2 appeared as the main constraint. Nevertheless, the use of CO_2 as a green solvent and a co-reagent used near single phase conditions, for electrochemical applications, remains of great interest, provided electrochemical conductivity problems are solved, for instance by an adapted geometry for the system of electrode.

References

[1] J.M. Dobbs, J.M. Wong, R.J. Lahiere, K.P. Johnson, Ind. Eng. Chem. Res. 26 (1987) 1476–1482.
[2] C.M. Cowey, K.D. Bartle, M.D. Burford, A.A. Clifford, S. Zhu, N.G. Smart, N.D. Tinker, J. Chem. Eng. Data 40 (1995) 1217–1221.
[3] A.C. Widrig, M.D. Porter, M.D. Ryan, T.G. Strein, A.G. Ewing, Anal. Chem. 62 (1990) 1R–20R.
[4] J. Golas, H.G. Drickamer, L.R. Faulkner, J. Phys. Chem. 95 (1991) 10191–10197.
[5] D. Niehaus, M. Philips, A. Michael, M.R. Wightman, J. Phys. Chem. 93 (1989) 6232–6236.
[6] M. Heintz, O. Sock, C. Saboureau, J. Périchon, Tetrahedron 44 (6) (1988) 1631–1636.
[7] J. Chaussard, M. Troupel, Y. Robin, G. Jacob, J.P. Juhasz, J. Appl. Electrochem. 19 (1989) 345–348.
[8] A. Savall, J. phys. IV 4(C1) (1994) 163–172.
[9] O. Sock, M. Troupel, J. Périchon, Tetrahedron Lett. 26 (12) (1985) 1509–1512.
[10] A. Sasaki, H. Kudoh, H. Senboku, M. Tokuda, Proceedings-International Symposium on Electroorganic Synthesis, third ed., 1997, pp. 245–247.
[11] S. Ching, R. Dudek, E. Tabet, J. Chem. Educ. 71 (7) (1994) 602–605.
[12] A.J. Bard, L.R. Faulkner, Electrochemical methods, second ed., Fundamentals and applications, John Wiley & Sons, Inc, 2001, pp. 226–260.
[13] A.M. Bond, Analyst 119 (1994) R1–R21.
[14] D. Giovanelli, N.S. Lawrence, R.G. Compton, Electroanalysis 16 (10) (2004) 789–810.
[15] G.S. Soave., Inst. Chem. Eng. Symp. Ser., 56 (1979), pp. 1.2/1–1.2/16.
[16] M.-J. Huron, J. Vidal, Fluid Phase Equilibr. 3 (1979) 255–271.
[17] M.L. Michelsen, Fluid Phase Equilibr. 60 (1990) 213–219.
[18] D.S. Abrams, J.M. Prausnitz, AIChE J. 21 (1975) 116–128.
[19] C. Duran-Valencia, A. Valtz, L.A. Galicia-Luna, D. Richon, J. Chem. Eng. Data 46 (2001) 1589–1592.
[20] S.R. Jacob, Q. Hong, B.A. Coles, R.G. Compton, J. Phys. Chem. B 103 (1999) 2963–2969.
[21] P. Cassoux, P. Dartiguepeyron, P.-L. Fabre, D. de Montauzon, Electrochim. Acta 30 (11) (1985) 1485–1490.
[22] B. Trémillon, Electrochimie Analytique et réactions en solution, Tome 2 –Réactions et méthodes électrochimiques, ed. Masson (1993) 79.

[23] R.M. Crooks, A.J. Bard, J. Electroanal. Chem. 243 (1988) 117–131.
[24] A.P. Abbott, T.A. Claxton, J. Fawcett, C.J. Harper, J. Chem. Soc. 12 (10) (1996) 435–440.
[25] A. Shariati, C.J. Peters, J. Supercrit. Fluid. 30 (2004) 139–144.
[26] H. Ohde, F. Hunt, S. Kihara, C.M. Wai, Anal. Chem. 72 (2000) 4738–4741.
[27] M.E. Philips, M.R. Deakin, M.V. Novotny, R.M. Wightman, J. Phys. Chem. 91 (1987) 3934–3936.
[28] S.A. Olsen, D.E. Tallman, Anal. Chem. 66 (1994) 503–509.
[29] S. Chanfreau, INPT Ph. D. Thesis (2005).